11. Spinelli E, Mauri T, Beitler JR, Pesenti A, Brodie D. Respiratory drive in the acute respiratory distress syndrome: pathophysiology, monitoring, and therapeutic interventions. *Intensive Care Med* 2020; 46:606–618.

Injury to the Endothelial Glycocalyx in Critically Ill Patients with COVID-19

To the Editor:

Severe acute respiratory syndrome coronavirus 2 (SARS-CoV-2) causes the so-called coronavirus disease (COVID-19), which is characterized by a broad spectrum of clinical presentations ranging from asymptomatic patients to critically ill individuals with a high case fatality rate (1). The critical care community has increasingly recognized that cardiovascular and thrombotic complications are relatively common in COVID-19 (2). Indeed, direct involvement of the vascular endothelium was recently reported in a series of patients suffering from severe COVID-19 (3). The endothelial glycocalyx (eGC), which covers the luminal surface of endothelial cells, contributes to the maintenance of vascular homeostasis, whereas disruption of the eGC is observed early in critically ill patients and is associated with inferior outcomes (4, 5).

Here, we investigated in translational human and cellular studies whether injury to the eGC can be found in critically ill patients with COVID-19 early after admission to the ICU. We collected plasma and serum from 19 adult individuals within 24 hours after invasive ventilation for acute respiratory distress syndrome and from 10 healthy human donors after written informed consent of patients or their legal representative. The first patient was admitted on March 19, 2020, and the observation period was until May 17, 2020. The median (interquartile range) observation duration was 47 (40–54) days.

Baseline patient characteristics at study inclusion as well as a description of the further clinical course are summarized in Table 1. Organ failure was not restricted to the lungs, and multiorgan dysfunction was common both at inclusion and during the further clinical course. Surprisingly, global markers of endothelial injury such as Angpt-1 (angiopoietin-1) (control: 29 [26.2–30.9] ng/ml vs. COVID-19: 27.8 [23.4–36.2] ng/ml; $P = 0.79$) and Angpt-2 (control: 0.655 [0.336–1.113] ng/ml vs. COVID-19: 0.434 [0.035–1.338] ng/ml; $P = 0.6$) were unchanged in patients with COVID-19. In contrast, marked increases in the soluble form of the sTie2 (Tie2 receptor) (Figure 1A) and in syndecan-1 (Figure 1B)—indicating pathological shedding of transmembrane proteins involved in glycocalyx structure and processing—were observed. The key eGC sheddase Hpa-1 (heparanase-1) and its enzymatic activity were both not significantly increased (data not shown). To the contrary, the Hpa-1 counterpart, the protective Hpa-2 (heparanase-2), was pertinently reduced in all patients with COVID-19 (Figure 1C). Driven by this acquired Hpa-2 deficiency, the Hpa-1:Hpa-2 ratio was higher in patients with COVID-19 ($P = 0.012$; data not shown). Together, this indicates that critically ill patients with COVID-19 suffer from an acquired Hpa-2 deficiency that can contribute to the degradation of the eGC, maybe even before classical endothelial activation and injury. Next, eGC structure was analyzed in humans, employing sublingual sidestream darkfield (SDF) imaging. We quantified the size of the individual patients' eGC using an indirect surrogate termed the perfused boundary region and found a decrease of perfused boundary region, indicating reduced eGC thickness in patients with COVID-19. To demonstrate that the deficiency of Hpa-2 is mechanistically involved in the degradation of the eGC, we used a microfluidic chamber with cultured endothelial cells (ECs) under flow that synthesize an intact and stable eGC under *in vitro* conditions. After stimulation with COVID-19 or control serum, the eGC was visualized by confocal microscopy followed by computerized three-dimensional reconstruction. Its thickness was then quantified by analyzing the heparan sulfate (HS)-positive area. We found that stimulation with COVID-19 was sufficient to severely damage the eGC (Figure 1E). The HS-positive area was reduced by 34% (control: $6.1 \pm 0.9\%$ vs. COVID-19: $4 \pm 0.4\%$ $P < 0.001$). Consistent with our observation in patients, we found that the transcription of Hpa-2 in COVID-19–stimulated ECs was significantly reduced after 6 hours (0.63 ± 0.02 relative expression to control; $P = 0.003$). Of note, transgenic overexpression of Hpa-2 in a lentivirus-transduced EC line was sufficient to reverse this phenotype, as the HS area in COVID-19 serum–treated lenti-control cells was $1.9 \pm 0.6\%$ but was $4.2 \pm 1.2\%$ in lenti-Hpa-2–overexpressing cells ($P < 0.001$). In other words, if ECs overexpress Hpa-2, the serum of patients with COVID-19 cannot degrade the eGC anymore.

This exploratory study has obvious limitations, most importantly, its small sample size and hypothesis-generating nature. Injury to the eGC is not a finding specific for COVID-19 but can be found in a wide range of critically ill patients (5). Because only a small selection of molecules that may participate in endothelial injury have been investigated in this study, we cannot exclude that further mediators may play a critical role in endothelial and eGC injury in patients with COVID-19. In addition, because of concerns of viral transmission, SDF imaging values could not be obtained from the same control patients from whom blood analysis was performed but were obtained from a separate historic in-center control cohort. Both control cohorts were not matched to the individual patients in terms of age, but the control group that blood was collected from was matched in terms of male predominance.

In summary, we found injury of the eGC and speculate that this might represent a potentially critical hallmark of later widespread endothelial injury in severe COVID-19. Reduced eGC thickness was visualized *in vivo* by employing sublingual SDF imaging in patients. At the same time, increased syndecan-1 and sTie-2 concentrations in the blood of these patients indicated shedding of important

S.D. is supported by the German Research Foundation (DA 1209/4-3) and the German Center for Lung Research.

Authors Contributions: K.S., P.A.G., B.S., T.W., H.H., M.M.H., and S.D. obtained retrospective data. K.S., P.A.G., A.B., and S.D. performed sidestream darkfield imaging measurements. P.A.G. and T.P. performed ELISA measurements, and Y.K. performed and analyzed flow measurements. K.S., P.A.G., H.H., T.W., M.M.H., and S.D. analyzed and discussed the data and generated figures and tables. K.S., P.A.G., and S.D. wrote the manuscript; all authors proofread the manuscript.

Originally Published in Press as DOI: 10.1164/rccm.202007-2676LE on August 24, 2020

Table 1. Patient Characteristics at Study Inclusion and Further Clinical Course

Characteristic	Results
Number of patients	19
Age, yr, median (interquartile range)	57 (45–69)
Sex, *n* (%)	
M	18 (95)
F	1 (5)
BMI, kg/m^2, median (interquartile range)	27.8 (26.2–33.5)
Comorbidities, *n* (%)	
Asthma	1 (5)
HTN	10 (53)
CHF	2 (11)
CAD	1 (5)
Diabetes	5 (26)
CKD	1 (5)
Obesity	7 (37)
Malignancy	2 (11)
Immunosuppression	2 (11)
Invasive ventilation, *n* (%)	19 (100)
Time from hospital to ICU admission, d, median (interquartile range)	0 (0–2)
Time from ICU admission to invasive ventilation, d, median (interquartile range)	0 (0–0)
Respirator parameters, median (interquartile range)	
$F_{I_{O_2}}$, %	50 (30–60)
PEEP, mbar	12 (12–15)
Pplat, mbar	27 (23–30)
Oxygenation index ($Pa_{O_2}/F_{I_{O_2}}$), mm Hg, median (interquartile range)	173 (152–260)
Pa_{CO_2}, mm Hg, median (interquartile range)	46 (40–51)
pH, median (interquartile range)	7.36 (7.32–7.41)
Lactate, mmol/L, median (interquartile range)	1.6 (1.5–2.9)
Vasopressor, *n* (%)	16 (84.2)
Norepinephrine dose, μg/kg/min, median (interquartile range)	0.083 (0.019–0.182)
Renal replacement therapy, *n* (%)	3 (16)
vv-ECMO support, *n* (%)	2 (11)
SOFA score, points, median (interquartile range)	11 (9–14)
Organ-specific failures, *n* (%)	
Respiratory ($Pa_{O_2}/F_{I_{O_2}} < 300$)	19 (100)
Coagulation (thrombocytes < 100)	1 (5)
Liver (bilirubin > 33 μmol/L)	1 (5)
Cardiovascular (dobutamine or norepinephrine)	16 (84)
Neurological (GCS < 13)	19 (100)
Renal (creatinine > 170 μmol/L)	4 (21)
Lab, median (interquartile range)	
CRP (normal: <5), mg/L	174 (121–203)
PCT normal: <0.5), μg/L	3.8 (0.5–10.9)
IL-6 (normal: <7), ng/L	272 (142–541)
LDH (normal: <248), U/L	548 (384–657)
D-Dimer (normal: <0.5), mg/L	3.56 (0.84–8.88)
Troponin T (normal: <14), ng/L	17 (11–23)
NT-proBNP (normal: <86), ng/L	260 (82–1108)
Further clinical course, *n* (%)	
Prone position	19 (100)
Inhaled NO	4 (21)
vv-ECMO	7 (37)
Renal replacement therapy	8 (42)
Septic shock	10 (53)
Died by end of observation period	3 (16)
Still dependent on critical care	6 (32)
Still dependent on mechanical ventilation	2 (11)

Definition of abbreviations: BMI = body mass index; CAD = coronary artery disease; CHF = congestive heart failure; CKD = chronic kidney disease; CRP = C-reactive protein; ECMO = extracorporeal membrane oxygenation; GCS = Glasgow Coma Scale; HTN = hypertension; LDH = lactate dehydrogenase; NT-proBNP = N-terminal pro–B-type natriuretic peptide; PCT = procalcitonin; PEEP = positive end-expiratory pressure; Pplat = plateau pressure; SOFA = Sequential Organ Failure Assessment; vv-ECMO = venovenous ECMO.

Demographic and clinical characteristics are given at the time of study inclusion as well as a description of the further clinical outcome within the observation period. Values are presented as median (interquartile range) or, if categorical, as numbers and percentages. Demographic characteristics for the control patients were as follows: age 32 (28–33) years and 9/10 male sex for laboratory investigation control patients; 39 (36–44) years and 5/10 male sex for sidestream darkfield imaging measurement control patients. All individuals of the control cohorts had no relevant medical preconditions.

endothelial transmembrane proteins responsible for building (5) and maintaining (6) the structure of the eGC, respectively. Interestingly, eGC shedding could be reproduced when patient blood was transferred *ex vivo* into an endothelial microcapillary chip model. Although Hpa-1 and its enzymatic activity (primarily responsible for HS degradation) (7) was found to be normal, Hpa-2, a protein that has been described as a protective antagonist of Hpa-1 (8, 9), was severely depleted in COVID-19. Importantly, degradation of the eGC after perfusion with COVID-19 serum could be attenuated in ECs overexpressing Hpa-2. We therefore postulate that acquired Hpa-2 deficiency might represent a potential mechanism of injury to the eGC, which could later progress to widespread endothelial dysfunction in COVID-19.

In conclusion, our data suggest that in critically ill patients with COVID-19, endothelial injury involves glycocalyx integrity, and acquired Hpa-2 deficiency might be a potential causative factor. ■

Author disclosures are available with the text of this letter at www.atsjournals.org.

Acknowledgment: The authors thank Yvonne Nicolai for excellent technical support and Dr. Markus Busch and Dr. Olaf Wiesner and the nursing staff for their infrastructural support in conducting this study.

Klaus Stahl, M.D.*
Phillip Alexander Gronski*
Yulia Kiyan, Ph.D.
Benjamin Seeliger, M.D.
Anna Bertram, M.D.
Thorben Pape
Tobias Welte, M.D.
Marius M. Hoeper, M.D.
Hermann Haller, M.D.
Hannover Medical School
Hannover, Germany

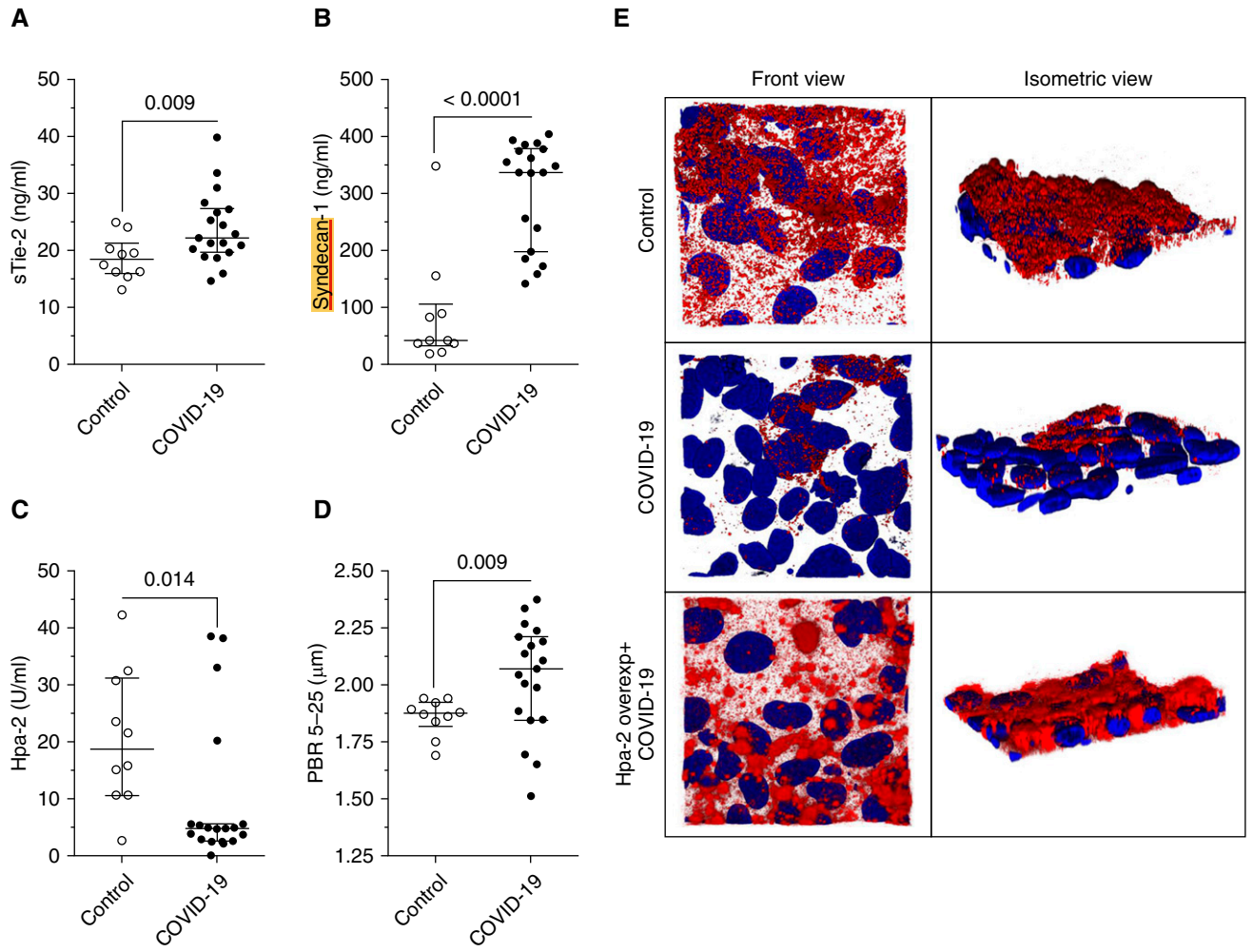

Figure 1. Injury to the endothelial glycocalyx in severe coronavirus disease (COVID-19). Scatter dot plots (median [interquartile range]) show (*A*) sTie-2 and (*B*) syndecan-1 concentrations for control and patients with COVID-19. Concentrations for both syndecan-1 (control: 41.5 [32.6–105.4] ng/ml vs. COVID-19: 336.5 [196.7–377.1] ng/ml) and sTie-2 (control: 18.4 [16–21.3] ng/ml vs COVID-19: 22.3 [19.7–27.3] ng/ml) were increased in patients with COVID-19. (*C*) Although both Hpa-1 (heparanase-1) concentration and activity were not significantly altered in comparison with control subjects, patients with COVID-19 showed an acquired deficiency in Hpa-2 (heparanase-2) (control: 18.7 [10.6–31.1] U/ml vs. COVID-19: 4.7 [2.6–5.1] U/ml). Consequentially, the Hpa-1: Hpa-2 ratio was higher in patients with COVID-19 (control: 0.08 [0.05–0.17] ng/U vs. COVID-19: 0.35 [0.27–0.66] ng/U). (*D*) Sidestream darkfield imaging in patients allows the quantification of endothelial glycocalyx thickness as indicated by increased perfused boundary region; this was increased in patients with COVID-19 (control: 1.9 [1.8–1.9] μm vs. COVID-19: 2.1 [1.8–2.2] μm), indicating reduced endothelial glycocalyx thickness. For comparison of groups, first, the normal distribution (D'Agostino-Pearson omnibus and Shapiro-Wilk normality test) of variables was tested, and then (*A* and *D*) two-sided unpaired *t* tests and (*B* and *C*) Mann-Whitney tests were used accordingly. (*E*) Exemplary three-dimensional reconstruction of the heparan sulfate (HS) layer images of naive endothelial cells in a microfluidic chip (HS in red; DAPI nuclei staining in blue) after perfusion with serum of a patient with COVID-19 (middle row) compared with a healthy control subject (upper row) in both front and isometric view angles demonstrates the diffuse loss of HS-rich glycocalyx layer in cells treated with COVID-19 serum. In Hpa-2–overexpressing endothelial cells (lower row), the HS surface layer is protected from injurious effects by perfusion with COVID-19 serum. overexp = overexpressing; PBR = perfused boundary region; sTie-2 = soluble Tie-2.

Sascha David, M.D.‡
Hannover Medical School
Hannover, Germany
and
University Hospital Zurich
Zurich, Switzerland

*These authors contributed equally to the manuscript and are both considered first authors.
‡Corresponding author (e-mail: sascha.david@usz.ch).

References

1. Bhatraju PK, Ghassemieh BJ, Nichols M, Kim R, Jerome KR, Nalla AK, *et al*. Covid-19 in critically ill patients in the seattle region: case series. *N Engl J Med* 2020;382:2012–2022.
2. Shi S, Qin M, Shen B, Cai Y, Liu T, Yang F, *et al*. Association of cardiac injury with mortality in hospitalized patients with COVID-19 in Wuhan, China. *JAMA Cardiol* 2020;5:802–810.
3. Varga Z, Flammer AJ, Steiger P, Haberecker M, Andermatt R, Zinkernagel AS, *et al*. Endothelial cell infection and endotheliitis in COVID-19. *Lancet* 2020;395:1417–1418.

4. Schmidt EP, Yang Y, Janssen WJ, Gandjeva A, Perez MJ, Barthel L, *et al*. The pulmonary endothelial glycocalyx regulates neutrophil adhesion and lung injury during experimental sepsis. *Nat Med* 2012;18:1217–1223.
5. Uchimido R, Schmidt EP, Shapiro NI. The glycocalyx: a novel diagnostic and therapeutic target in sepsis. *Crit Care* 2019;23:16.
6. Lukasz A, Hillgruber C, Oberleithner H, Kusche-Vihrog K, Pavenstädt H, Rovas A, *et al*. Endothelial glycocalyx breakdown is mediated by angiopoietin-2. *Cardiovasc Res* 2017;113:671–680.
7. Martin L, Koczera P, Zechendorf E, Schuerholz T. The endothelial glycocalyx: new diagnostic and therapeutic approaches in sepsis. *BioMed Res Int* 2016;2016:3758278.
8. Levy-Adam F, Feld S, Cohen-Kaplan V, Shteingauz A, Gross M, Arvatz G, *et al*. Heparanase 2 interacts with heparan sulfate with high affinity and inhibits heparanase activity. *J Biol Chem* 2010;285: 28010–28019.
9. Kiyan Y, Tkachuk S, Kurselis K, Shushakova N, Stahl K, Dawodu D, *et al*. Heparanase-2 protects from LPS-mediated endothelial injury by inhibiting TLR4 signalling. *Sci Rep* 2019; 9:13591.

Venoarterial Extracorporeal Membrane Oxygenation Support Rescue of Obstructive Shock Caused by Bulky Compressive Mediastinal Cancer

To the Editor:

Over the last decade, venoarterial extracorporeal membrane oxygenation (VA-ECMO) has increasingly been used in the setting of cardiogenic shock because it provides both respiratory and cardiac support, is easy to implant at the bedside by trained operators, and could, therefore, restore multiorgan perfusion. Despite no randomized controlled trials and few data on long-term quality of life in these patients, VA-ECMO has emerged as the first-line temporary cardiac support, with a growing number of accepted indications. Beyond classical medical indications, such as acute myocardial infarction, myocarditis, drug-induced cardiotoxicity, and end-stage dilated cardiomyopathy, VA-ECMO salvage therapy for obstructive cardiogenic shock caused by bulky malignancies is a rare emerging indication. Meanwhile, recent reports on critically ill patients with life-threatening malignancy-related complications suggested that urgent chemotherapy could be initiated with appreciable benefits on outcome (1–4).

We describe a recent case series of five patients rescued by VA-ECMO support combined with urgent chemotherapy for obstructive cardiogenic shock that revealed tumoral mediastinal syndrome. These young patients (median age, 23 yr) had no remarkable medical history and complained of dyspnea ($n = 5$), chest pain ($n = 2$) and/or chest swelling ($n = 2$) several days before suddenly worsening (Table 1). At ICU admission, they had severe obstructive cardiogenic shock with multiorgan failure (median Sequential Organ Failure Assessment score, 14) and cardiac arrest ($n = 2$) requiring emergency VA-ECMO rescue. Peripheral lymph nodes ($n = 2$) or superior vena cava syndrome ($n = 2$) associated with severe cardiogenic shock of unknown origin led to echocardiography and thoracic computed tomographic scans. Imaging findings included bulky mediastinal tumors compressing the right ventricle outflow tract, pulmonary infundibulum, main pulmonary arteries, and/or superior vena cava. After stopping heparin for at least 4 hours and ensuring a platelet count $>100 \times 10^9$/L and a fibrinogen level $>2 \times 10^9$/L, histological examination of lymph node or computed tomography–guided tumor biopsies obtained on ECMO from all patients provided diagnoses of diffuse large B-cell lymphoma (three patients), adult T-cell acute lymphoblastic lymphoma (one patient), and poorly differentiated carcinoma (one patient). Two patients had a hemorrhagic shock after the biopsy (i.e., patients 2 and 3) managed without arterial embolization. Four patients received urgent debulking chemotherapy; the last patient died of multiorgan failure before treatment could be started. Chemotherapy regimens targeting lymphoma included rituximab (in diffuse large B-cell lymphomas), cyclophosphamide, doxorubicin, vincristine, and/or prednisone (Table 1). The ensuing tumor reduction allowed successful ECMO withdrawal after a median of 12.5 days. Figure 1 illustrates patient 1's sequential imaging from the start of ECMO to Day 15. The four treated patients survived to ICU discharge after medians of 3 days on mechanical ventilation and 15 days in the ICU. They were then transferred to the hematology center. All were alive 3 months after ICU admission. The most frequent ECMO-related complication, cannula-site infection, occurred in three patients and was successfully treated.

Obstructive cardiogenic shock secondary to bulky mediastinal malignancies represents a rare but potentially fatal entity. For hemodynamic instability and multiorgan failure, salvage VA-ECMO seems to be the first option to immediately restore organ perfusion, thereby providing time to diagnose the underlying cause and start urgent chemotherapy. Despite the small number of patients reported, our case series supports VA-ECMO feasibly in this context and indicates that it should be initiated early because rapid implantation of the system and prompt diagnosis are decisive for therapeutic success.

The global prognoses of patients with hematological malignancies and solid cancers have improved dramatically over the past two decades, leading to growing numbers of them being admitted to the ICU and better post-ICU outcomes (5–7). To achieve a better outcome, identifying patients who are more likely to benefit from invasive organ supports, such as ECMO, is crucial. This has been already reported in cases in which immunocompromised patients may require extracorporeal life support because of severe refractory acute respiratory distress syndrome secondary to primary or opportunistic lung infections, drug-related organ toxicity, or specific infiltration from the underlying malignancy. Interestingly, when compared with patients from other immunocompromised categories, patients with hematological malignancies had a dismal prognosis, with worse outcomes reported for patients with leukemia/allogenic hematopoietic stem-cell transplants compared with patients with lymphoma (8). Even if the prognosis and the management of cardiogenic shock strongly differs with acute respiratory distress syndrome, ECMO should also be restricted to patients with realistic oncological/therapeutic prognoses, acceptable functional status, and few pre-ECMO mortality-risk factors. Similar management and wise patient selection are therefore warranted in the context of

Originally Published in Press as DOI: 10.1164/rccm.202001-0193LE on June 16, 2020